City, University of London Institutional Repository

This is the accepted version of the paper.

This version of the publication may differ from the final published version.

Third-order statistical linearization-based approach to derive equivalent linear properties of bilinear hysteretic systems for seismic response spectrum analysis

Pol D Spanos*

L.B. Ryon Chair in Engineering
Rice University
6100 Main, Houston, TX 77005, USA
e-mail: spanos@rice.edu
tel: 001-713 348 4909

Agathoklis Giaralis

Lecturer in Structural Engineering
School of Engineering and Mathematical Sciences
City University London
Northampton Square, EC1V 0HB, London, UK
e-mail: agathoklis.giaralis.1@city.ac.uk

Abstract

A novel statistical linearization based approach is proposed to derive effective linear properties (ELPs), namely damping ratio and natural frequency, for bilinear hysteretic SDOF systems subject to seismic excitation specified by an elastic response/design spectrum. First, an efficient numerical scheme is used to derive a power spectrum satisfying a certain statistical compatibility criterion with the given response spectrum. Next, the thus derived power spectrum is used in conjunction with a frequency domain higher-order statistical linearization formulation to replace the bilinear hysteretic system by a third order linear system by minimizing an appropriate error function in the least square sense. Then, this third-order linear system is used to derive a second order linear oscillator possessing a set of ELPs by enforcing equality of certain response statistics of the two linear systems. The thus derived ELPs, are utilized to estimate the peak response of the considered nonlinear system in the

context of linear response spectrum-based dynamic analysis. In this manner the need for numerical integration of the nonlinear equation of motion is circumvented. Numerical results pertaining to the European EC8 uniform hazard elastic response spectrum are presented to demonstrate the applicability and the usefulness of the proposed approach. These are further supported by Monte Carlo analyses involving an ensemble of 250 non-stationary artificial EC8 spectrum compatible accelerograms. It is believed that the proposed approach can be an effective tool in the preliminary aseismic design stages of yielding structures following either a force-based or a displacement-based methodology.

1. Introduction

Aseismic code provisions define seismic severity via elastic uniform hazard spectra derived from probabilistic seismic hazard analysis (e.g. [1]) associated with the peak response of linear viscously damped single-degree-of-freedom (SDOF) oscillators. However, ordinary structures are designed to behave inelastically (i.e. to suffer structural damage) for the prescribed "design" seismic severity level. To account for this nonlinear/hysteretic behavior within a response spectrum-based analysis framework, inelastic design spectra of reduced coordinates by a strength reduction factor R are usually prescribed by regulatory agencies (e.g. [2,3]). These spectra provide the peak response of hysteretic SDOF systems with T_n natural period of small oscillations. The development of inelastic spectra relies either on a straightforward computation of the peak inelastic deformation or on R-μ-T_n relations, where μ is the ductility ratio. In both cases comprehensive Monte Carlo analyses involving numerical integration of the nonlinear equations governing the motion of the hysteretic systems exposed to ensembles of field recorded seismic accelerograms are required (e.g. [4,5]).

Alternatively, approximate linearization techniques can be used to study the response of nonlinear systems (see e.g. [6-9] and references therein). These techniques approximate the peak inelastic response by considering the peak response of an equivalent linear SDOF oscillator (ELS) characterized by effective linear properties (ELPs), that is, damping ratio and natural frequency. A plethora of hysteretic constitutive laws is available. Nevertheless, the simple bilinear hysteretic law is the most extensively considered in such studies. Further, it is the most commonly assumed model in the everyday practice of earthquake resistant design of yielding structures. Most of the existing studies in the literature assume deterministic harmonic input to derive ELPs by averaging various quantities of interest over one cycle of the hysteretic response (e.g. [7,8]). Herein a recently proposed by the authors [10,11] statistical linearization based approach which is not restricted by the aforementioned limitation is extended to derive ELPs from bilinear hysteretic SDOF systems associated with any given elastic response spectrum. Notably, this is achieved without resorting to computationally demanding integration of the underlying nonlinear equation of motion. Furthermore, the need to select and scale accelerograms compatible with the given response spectrum is also circumvented.

The adopted linearization approach seeks, first, a "quasi-stationary" stochastic seismic excitation process of finite duration derived via a computationally efficient numerical scheme to achieve compatibility with a given elastic (uniform hazard) response spectrum in a statistical sense. This process is defined in the frequency domain by means of a non-parametric power spectrum. Next, the thus derived power spectrum is treated as the input spectrum to perform statistical linearization [12]. In this manner, an equivalent linear SDOF oscillator is determined whose properties depend both on the nonlinear system and on the given response spectrum.

In [10, 11] an early statistical linearization formulation [13] assuming Gaussian narrow-band response of the considered nonlinear system and relying on stochastic averaging over one period of oscillation has been sought to derive a second order ELS corresponding to a linear SDOF oscillator. Herein, an efficient frequency-domain statistical linearization solution procedure is formulated which replaces the bilinear hysteretic system by a third order linear system [14]. This statistical linearization formulation is based on less restrictive assumptions than the one adopted in [11] allowing for the treatment of bilinear hysteretic oscillators exhibiting strong nonlinear behavior (see also [12,15,16]). However, the thus derived third order ELS does not correspond to any particular physical system and cannot be readily related to a response spectrum pertaining to the peak response of linear SDOF oscillators. To this end, a novel step is introduced herein which considers an effective second order linear oscillator obtained by enforcing equality of its displacement and velocity response variances with those of the third order ELS. The reduced-order effective linear system corresponds to a SDOF linear oscillator characterized by an effective damping ratio and an effective natural frequency (ELPs). These properties are then used in conjunction with design spectra defined for various damping ratios to estimate the peak response of the underlying bilinear hysteretic oscillator.

It is noted that the purpose of this work is not to propose an accurate statistical linearization formulation for the estimation of the peak response of nonlinear systems. This issue has been previously addressed in the literature by various researchers (e.g. [17,18]). Herein, the objective is to propose a computationally efficient approach for the task which can be readily incorporated in the everyday engineering practice to facilitate aseismic structural design at a preliminary stage. Statistical linearization is used as a "step" to achieve this goal. This point is further clarified in Fig. 1 which presents a flowchart of the proposed approach comprising three steps (circled). These include: a) The derivation of a response

spectrum compatible power spectrum (an efficient method to accomplish this task is reviewed in Section 2 based on the work of Vanmarcke [19] and Cacciola et al. [20], though other methods for the purpose exist in the literature (e.g. [21,22]), b) The application of statistical linearization to obtain a third order linear system (a formulation due to Asano and Iwan [14] is utilized as detailed in Section 3), and c) The reduction of the third-order linear system to a second-order linear SDOF system corresponding to a linear oscillator (section 4 introduces a novel statistical criterion for this task). Furthermore, section 5 discusses certain practical issues of using the effective linear properties characterizing the derived linear SDOF oscillator to estimate the peak nonlinear response of bilinear hysteretic systems from heavily damped response spectra. Further, section 6 provides numerical data pertaining to various bilinear hysteretic SDOF systems exposed to the elastic uniform hazard spectrum prescribed by the European aseismic code provisions [2] to demonstrate the effectiveness and applicability of the proposed approach. Finally, section 7 includes pertinent concluding remarks.

Fig. 1 Flowchart of the proposed approach.

$S_a(T,\zeta)$: Elastic response spectrum for various damping ratios ζ

Solution of an inverse stochastic dynamics problem

$G(\omega)$: Response spectrum compatible "quasi"-stationary power spectrum for damping ratio ζ_n

Bilinear SDOF system with viscous damping ratio ζ_n and pre-yield natural period T_n

Higher-order Statistical Linearization

Third-order equivalent linear system

Order reduction via a statistical criterion

T_{eff} and ζ_{eff}: effective linear properties characterizing a linear SDOF oscillator

$S_a(T_{eff}, \zeta_{eff})$:
Peak response of the bilinear system obtained from the elastic response spectrum

Fig. 1 Flowchart of the proposed approach.

2.   Derivation of response spectrum compatible finite duration stationary stochastic processes

Field recorded acceleration traces of strong ground motions associated with historic seismic events exhibit a time-decaying intensity after the initial period of growth. In many cases a well-defined time window of constant fully-developed intensity is observed in between the initial build-up and the final decaying parts of these time-histories. This observation has led several researchers to consider the representation of seismic action by means of a "quasi-stationary" zero-mean Gaussian acceleration stochastic process $g(t)$ of finite duration T_s corresponding to the width of the aforementioned window (see e.g. [19,22-24]). This process is conveniently represented in the domain of frequencies ω by a one-sided power spectrum $G(\omega)$. In relating $G(\omega)$ to a response spectrum the response statistics of a linear single-degree-of-freedom (SDOF) system with natural frequency ω_j and ratio of critical damping ζ base-excited by the process $g(t)$ need to be considered. These statistics can be expressed in terms of the spectral response moments of order m of the SDOF system given by the equation (e.g. [25])

$$\lambda\left(T_s\right)_{j,m,G} = \lambda_{j,m,G} = \int_0^\infty \omega^m G(\omega)\left|H\left(\omega,T_s\right)\right|^2 d\omega .$$ (1)

In the above equation, $H(\omega,T_s)$ is the time-dependent transfer function of the considered system evaluated at a time equal to the duration of $g(t)$. For the purposes of this study, the following mathematically convenient approximate formula is adopted for the squared modulus of this transfer function [19]

$$\left|H\left(\omega,T_s\right)\right|^2 \approx \frac{1}{\left(\omega_j^2 - \omega^2\right)^2 + \left(2\zeta_j\omega_j\omega\right)^2} ,$$ (2)

where

$$\zeta_j = \frac{\zeta}{1 - \exp\left(-2\zeta\omega_j T_s\right)} .$$ (3)

The latter quantity is a fictitious duration-dependent ratio of critical damping to account for the fact that the response statistics of relatively lightly damped flexible SDOF oscillators may not reach their stationary (steady-state) values if the duration T_s is not long enough [19,22-27]. Note that for $\zeta_j = \zeta$ Eq. (2) coincides with the squared modulus of the well-known stationary transfer function of linear SDOF systems. In this case, Eq. (1) provides the response statistics of SDOF oscillators as if $g(t)$ were a stationary process of infinite duration. In Fig. 2 the ratio ζ_j/ζ is plotted versus the natural period of oscillation $T = 2\pi/\omega_j$ for several damping ratios ζ and durations T_s to quantify numerically when the "corrective" damping ζ_j of Eq.(3) becomes important in the evaluation of the response statistics of linear SDOF systems.
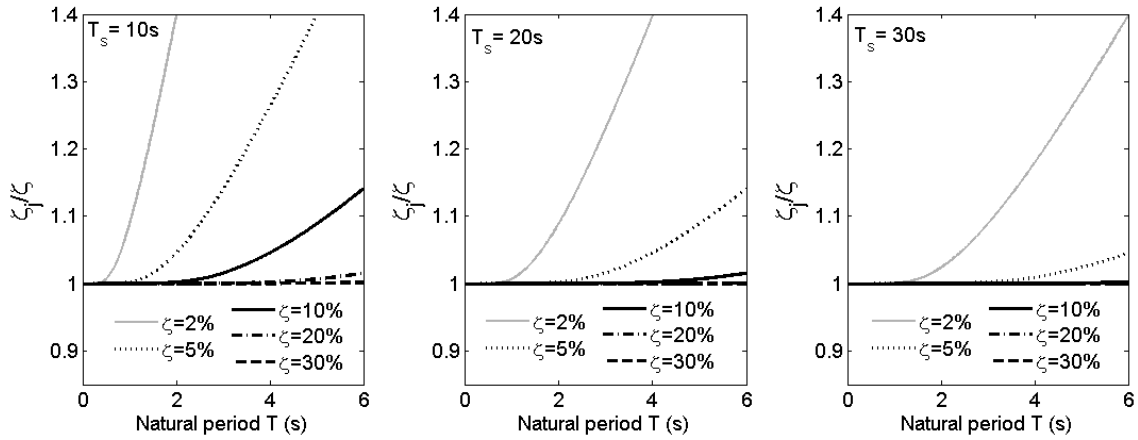
Fig. 2 Influence of duration T_s, damping ζ, and natural period $T = 2\pi/\omega_j$ on the ratio ζ_j/ζ.

Let $S_a(T,\zeta)$ denote an elastic response pseudo-acceleration seismic spectrum. The concept of a "peak factor" η_j can be used to establish a relation between S_a and the power spectrum $G(\omega)$ by relying on the equation [19]

$$S_a\left(\frac{2\pi}{\omega_j},\zeta\right) = \eta_j \omega_j^2 \sqrt{\lambda_{j,0,G}}. \tag{4}$$

In this regard, η_j can be defined as the ratio of the peak over the standard deviation $\sigma = (\lambda_{j,0,G})^{1/2}$ of the response deformation of a SDOF oscillator excited by $g(t)$ evaluated at $t = T_s$.

The exact determination of the peak factor requires a closed-form solution of the first passage problem of stochastically excited systems, namely what is the time instant for the response of the considered oscillator to reach/cross a specific level of intensity with probability p; no such solution is available in the literature. However, several researchers have proposed various semi-empirical expressions to obtain reliable estimates of the peak factor for various input stochastic processes (e.g. [19,24,28,29]). In determining the peak factor η_j appearing in Eq. (4) the following approximate semi-empirical expression is adopted herein [19]

$$\eta_j = \sqrt{2\ln\left\{2v_j\left[1-\exp\left(-q_j^{1.2}\sqrt{\pi\ln\left(2v_j\right)}\right)\right]\right\}},$$
(5)

where

$$v_j = \frac{T_s^*}{2\pi}\sqrt{\frac{\lambda_{j,2,G}}{\lambda_{j,0,G}}}\left(-\ln p\right)^{-1},$$
(6)

and

$$q_j = \sqrt{1-\frac{\lambda_{j,1,G}^2}{\lambda_{j,0,G}\lambda_{j,2,G}}}.$$
(7)

Furthermore, the symbol T_s^* in Eq. (6) denotes a reduced "equivalent stationary response" duration which takes into account the transient nature of $g(t)$ [19]. It is given by the following expression

$$T_s^* = T_s\exp\left(-2\left(\frac{\lambda\left(T_s\right)_{j,0,G}}{\lambda\left(T_s/2\right)_{j,0,G}}-1\right)\right).$$
(8)

The ratio T_s^*/T_s depends on the duration T_s and on the properties of the considered SDOF oscillator in a similar manner as the ratio ζ_j/ζ. Specifically, as the product $\zeta\omega_j T_s$ increases the ratio of the transient response variances included in Eq. (8) will tend to unity and thus $T_s^* \rightarrow T_s$. Note in passing that other approaches to estimate the peak factor for non-stationary excitations have also been proposed in the literature (e.g. [28,29]). The herein approach due to Vanmarcke [19] has been adopted due to its relative simplicity which serves well the practical nature of the present work.

By setting $p = 0.5$ in Eq. (6) the rhs of Eq. (4) estimates the level of the peak pseudo-acceleration response of a SDOF oscillator excited by the process $g(t)$ not to be exceeded with probability 50%. Therefore, S_a becomes the median pseudo-acceleration response spectrum satisfying the following criterion: considering an ensemble of realizations of the process $g(t)$, half of the population of their response spectra will lie below S_a [19]. Given a (target) response spectrum S_a, a non-parametric estimate of the power spectrum $G(\omega)$ conforming with the aforementioned criterion can be recursively evaluated at a specific set of N equally spaced natural frequencies $\omega_k = \omega_0 + (k-0.5)\Delta\omega$; $k = 1,2,\ldots,N$. This is achieved by using the equation [11,20]

$$G[\omega_k] = \begin{cases} \dfrac{4\zeta_k}{\omega_k \pi - 4\zeta_k \omega_{k-1}} \left(\dfrac{S_a^2 \left(2\pi / \omega_k, \zeta \right)}{\eta_k^2} - \Delta\omega \sum_{i=1}^{k-1} G[\omega_i] \right); \omega_0 < \omega_k \leq \omega_N \\ 0 \, ; 0 \leq \omega_k \leq \omega_0 \end{cases}. \tag{9}$$

In the last equation, ω_N is a "cut-off" frequency above which $G(\omega)$ attains negligible values. Furthermore, ω_0 is the lowest value of natural frequency for which Eq. (5) is defined, namely [11]

$$\omega_0 = \min_{\omega_k} \left\{ \ln \left\{ 2v_k \left[1 - \exp\left(-q_k^{1.2} \sqrt{\pi \ln(2v_k)} \right) \right] \right\} \geq 0 \right\}. \tag{10}$$

In implementing the recursive numerical scheme defined by Eq. (9) a stochastic process different than the (unknown) $G(\omega)$ needs to be assumed to evaluate the peak factors η_k. For this task, a viable candidate is a stationary white noise. Under this assumption, the peak factors η_k appearing in Eq. (9) can be determined by substituting in Eq.(5) [24]

$$v_k = -\frac{T_s}{2\pi \ln(0.5)} \omega_k, \tag{11}$$

and

$$q_k = \sqrt{1 - \frac{1}{1 - \zeta^2} \left(1 - \frac{2}{\pi} \tan^{-1} \frac{\zeta}{\sqrt{1 - \zeta^2}} \right)^2}. \tag{12}$$

Upon determining the discrete power spectrum $G[\omega]$ at ω_k frequencies by Eq. (9), the associated pseudo-acceleration response spectrum $D[\omega_k,\zeta]$ can be approximated using Eqs. (1)~(8). This task involves the evaluation of the first three response spectral moments which can be efficiently accomplished by the formulae included in the Appendix A [30]. One can then compare the thus obtained spectrum D with the target spectrum S_a to assess the error induced by the various approximations discussed above. In this respect, extensive numerical experimentation, not included herein for brevity, has shown that for a damping ratio $\zeta=5\%$, which is the most common value adopted in earthquake resistant design applications, and for durations $T_s \geq 15$s, the stationary assumption in the evaluation of the peak factors η_k has a negligible impact on the effectiveness of Eq. (9) in yielding power spectra compatible with the target spectrum S_a. However, for lower damping values and/or shorter durations the transient nature of the assumed white noise process needs to be accounted for. This can be achieved by substituting in Eq. (12) the duration-dependent damping of Eq. (3) and by using the reduced duration T_s^* in Eq. (11) given, in the case of white noise, by the expression [19]

$$T_s^* = T_s \exp\left(-2\left(\frac{1-\exp(-2\zeta\omega_k T_s)}{1-\exp(-\zeta\omega_k T_s)}-1\right)\right).\qquad (13)$$

. The estimate of G obtained by Eqs. (9-12) using the white noise approximation may then be modified iteratively to improve the point-wise matching of the response spectrum $D[2\pi/\omega_k,\zeta]$ with the target spectrum by means of the following equation written at the M-th iteration [11, 22]

$$G^{(M+1)}[\omega_k] = G^{(M)}[\omega_k]\left(\frac{S_a[2\pi/\omega_k,\zeta]}{D^{(M)}[2\pi/\omega_k,\zeta]}\right)^2.\qquad (14)$$

In this manner, excellent accuracy between D and S_a is achieved within three to four iterations [11].

As a final note of practical interest it is pointed out that the value of the assumed duration T_s will in general influence the response spectrum compatible power spectrum $G(\omega)$ as obtained from Eqs. (9) and (14). In dealing with response spectra corresponding to a specific field recorded accelerogram, T_s has the physical meaning of the time window corresponding to the "stationary" strong part of the ground motion as noted in the beginning of this section. In such cases, the choice of T_s requires careful consideration to represent realistically the underlying strong ground motion [22]. However, in this work the target response spectrum S_a is a "design" Uniform Hazard Spectrum (UHS) which does not correspond to any physical accelerogram. In this context, the process $g(t)$ defined by its frequency domain representation $G(\omega)$ can be construed as a mathematical tool to represent the UHS spectrum in a convenient manner that allows for the application of statistical linearization as detailed in the following sections. Therefore, it is recommended to adopt a sufficiently large value for T_s depending on the considered damping ratio ζ to facilitate the numerical work involved in determining effective linear properties according to the proposed approach outlined in Fig. 1. To this aim, the data presented in Fig. 2 can serve as a guide for choosing appropriately the duration T_s; this point will be further elucidated in subsequent sections.

The next step of the herein proposed methodology is to utilize the design spectrum compatible power spectrum $G[\omega_k]$ obtained from Eqs. (9) or (14) in conjunction with the method of statistical linearization. This will lead to the determination of a third-order linear system associated with a specific bilinear hysteretic oscillator. The mathematical details of this step are described in the next section.

3. Frequency-domain statistical linearization solution for bilinear hysteretic systems

The inelastic behavior of yielding structures subject to strong ground motions is commonly modeled in various earthquake resistant design approaches by means of bilinear hysteretic viscously damped SDOF systems (e.g. [3,31]). The dynamic behavior of such a system is fully characterized by the following five properties: mass m, viscous damping coefficient c, pre-yield stiffness k, rigidity α (ratio of the post-yield over the pre-yield stiffness), and yielding deformation x_y. Shown in Fig. 3(a) is a mechanical representation of the considered system base excited by the acceleration process $g(t)$ [14]. It consists of two springs, a dashpot, and a Coulomb friction element which slips when the exerted force becomes greater than $(1-\alpha)kx_y$. A graph of the restoring force of the depicted system for zero damping is shown in Fig. 3(b) along with the definitions of certain response quantities of practical interest in the aseismic structural design (i.e. the strength reduction factor R and the ductility ratio μ). The motion of the bilinear hysteretic system of Fig. 3(a) is governed by the following system of differential equations with zero initial conditions [14,16]

$$\ddot{x}(t)+2\zeta\omega_n\dot{x}(t)+a\omega_n^2 x(t)+\omega_n^2(1-a)f_1\big(\dot{x}(t),z(t),x_y\big)=-g(t), \tag{15}$$

$$\dot{z}(t)=\dot{x}(t)f_2\big(\dot{x}(t),z(t),x_y\big), \tag{16}$$

where

$$
\begin{aligned}
f_1\big(\dot{x}(t),z(t),x_y\big)&=z(t)f_2\big(\dot{x}(t),z(t),x_y\big)\\
&+x_y\big(U\{z(t)-x_y\}U\{\dot{x}(t)\}-U\{-z(t)-x_y\}U\{-\dot{x}(t)\}\big)
\end{aligned}\tag{17}
$$

and

$$f_2\big(\dot{x}(t),z(t),x_y\big)=\big(1-U\{z(t)-x_y\}U\{\dot{x}(t)\}-U\{-z(t)-x_y\}U\{-\dot{x}(t)\}\big). \tag{18}$$

In the above equations ω_n is the pre-yielding natural frequency of the considered system, x is its response displacement process relative to the motion of the ground (deformation), and z is an additional "state" corresponding to the relative displacement of the Coulomb friction element as indicated in Fig. 3 [14]. Further, in the previous equations and hereafter, the dot over a symbol denotes differentiation with respect to time, and $U\{\cdot\}$ is the Heaviside step function, that is, $U\{v\}=1$ for $v \geq 0$, and $U\{v\}=0$ for $v<0$.
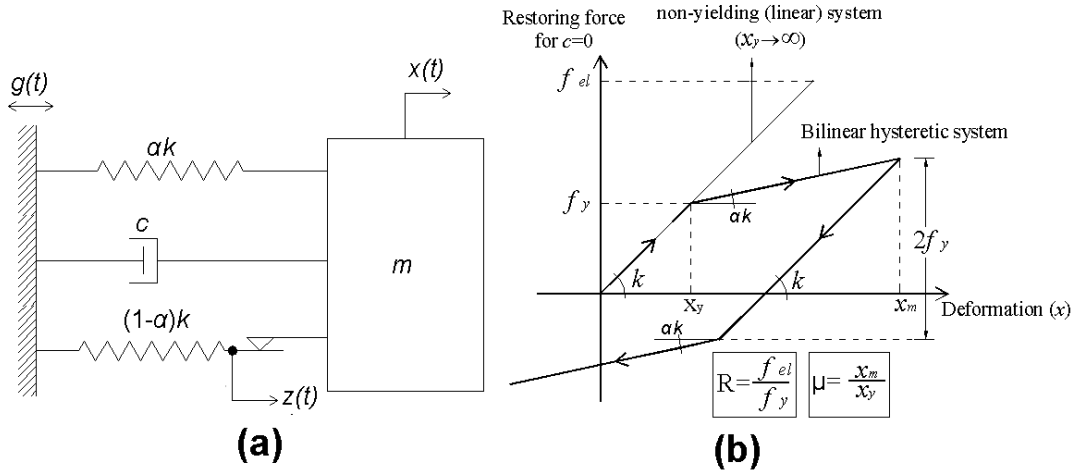
Fig. 3 (a) Mechanical representation of a bilinear hysteretic SDOF system (b) Bilinear Restoring force-deformation and definitions of the strength reduction factor R and ductility μ.

It is noted that the expression in Eq. (17) ensures that z is bounded within the $[-x_y, x_y]$ interval and thus the restoring force from the Coulomb element lies within $\pm(1-a)kx_y$ [14,16]. Furthermore, the consideration of the z state renders it possible to mathematically express the bilinear perfectly elasto-plastic hysteretic behavior, corresponding to $\alpha=0$, via the first order differential equation Eq. (16) [32]. The latter equation reflects that the rate of change of z is equal to $\dot{x}$ (no slip occurs) for $|z|<x_y$ and becomes zero for $|z|=x_y$. More importantly, the consideration of the z state allows for the employment of a statistical linearization scheme proposed to treat stochastically excited non-linear multi-degree-of-freedom structural systems [12,33], based on the early work of Kazakov [34]. Application of this statistical linearization

scheme to the system of the non-linear Eqs. (15) and (16) yields the system of linear differential equation [14]

$$\ddot{x}(t) + 2\zeta\omega_n \dot{x}(t) + a\omega_n^2 x(t) + \omega_n^2 (1-a)(C_1\dot{x}(t) + C_2 z(t)) = -g(t) \tag{19}$$

and

$$\dot{z}(t) + C_3\dot{x}(t) + C_4 z(t) = 0. \tag{20}$$

The four equivalent linear coefficients C_1 to C_4 appearing in the last two equations are determined by requiring minimization of the mean square error in replacing Eqs. (15) and (16) by Eqs. (19) and (20), respectively [12]. Implementing the procedure delineated in [12] the following expressions for the aforementioned coefficients are derived

$$C_1 = E\left\{\frac{\partial f_1(\dot{x}(t), z(t), x_y)}{\partial \dot{x}(t)}\right\} =$$
$$-\frac{\sigma_z\sqrt{1-\rho^2}}{\pi\sigma_{\dot{x}}}\exp\left(\frac{-x_y^2}{2\sigma_z^2(1-\rho^2)}\right) + \frac{x_y}{\sqrt{2\pi}\sigma_{\dot{x}}\sigma_z\sqrt{1-\rho^2}}\mathrm{erfc}\left(\frac{x_y}{\sigma_z\sqrt{2(1-\rho^2)}}\right), \tag{21}$$

$$C_2 = E\left\{\frac{\partial f_1(\dot{x}(t), z(t), x_y)}{\partial z(t)}\right\} =$$
$$\frac{1}{2}\left[1 + \mathrm{erf}\left(\frac{x_y}{\sigma_z\sqrt{2}}\right)\right] - \frac{1}{\sqrt{\pi}}\int_{\frac{x_y}{\sigma_z\sqrt{2}}}^{\infty}\exp(-v^2)\mathrm{erf}\left(\frac{\rho v}{\sqrt{1-\rho^2}}\right)dv, \tag{22}$$

$$C_3 = -E\left\{\frac{\partial[\dot{x}(t)f_2(\dot{x}(t), z(t), x_y)]}{\partial \dot{x}(t)}\right\} = -C_2, \tag{23}$$

and

$$C_4 = -E\left\{\frac{\partial[\dot{x}(t)f_2(\dot{x}(t), z(t), x_y)]}{\partial z(t)}\right\} =$$
$$\frac{\rho x_y \sigma_{\dot{x}}}{\sigma_z^2\sqrt{2\pi}}\exp\left(\frac{-x_y^2}{2\sigma_z^2}\right)\left[1 + \mathrm{erf}\left(\frac{\rho x_y}{\sigma_z\sqrt{2(1-\rho^2)}}\right)\right] + \frac{\sigma_{\dot{x}}\sqrt{1-\rho^2}}{\pi\sigma_z}\exp\left(\frac{-x_y^2}{2(1-\rho^2)\sigma_z^2}\right), \tag{24}$$

in which

$$\sigma_{\dot{x}}^2 = E\left\{\dot{x}(t)^2\right\}; \sigma_z^2 = E\left\{z(t)^2\right\}; \rho = \frac{E\left\{\dot{x}(t)z(t)\right\}}{\sigma_z \sigma_{\dot{x}}}. \tag{25}$$

In the previous equations and henceforth $E\{\cdot\}$ denotes the mathematical expectation operator. Moreover, $erf(\cdot)$ and $erfc(\cdot)$ are the standard error and complementary error functions defined by the expressions

$$erf(u) = \frac{2}{\sqrt{\pi}} \int_0^u \exp\left(-w^2\right) dw; erfc(u) = 1 - erf(u). \tag{26}$$

From the Eqs. (21) to (25) it is seen that the equivalent linear coefficients C_1 to C_4 to be determined depend on the variance of the processes $\dot{x}$ and z, that is $\sigma_{\dot{x}}^2$ and σ_z^2, and on their cross-variance $E\{\dot{x}z\}$. To this end, an efficient frequency domain formulation relying on the spectral input/output relations for linear systems is used to calculate these response moments [35]. This formulation is significantly different from the state-space approach commonly considered in the literature for the purpose [14,16]. It facilitates the numerical implementation of the herein considered approach in which the input spectrum $G(\omega)$ is given in a non-parametric form known at discrete frequencies as explained in the previous section. Specifically, the system of Eqs. (19) and (20) is first written in matrix form as

$$\mathbf{M}\begin{Bmatrix}\ddot{x}(t) \\ \ddot{z}(t)\end{Bmatrix} + \mathbf{C}\begin{Bmatrix}\dot{x}(t) \\ \dot{z}(t)\end{Bmatrix} + \mathbf{K}\begin{Bmatrix}x(t) \\ z(t)\end{Bmatrix} = \begin{Bmatrix}-g(t) \\ 0\end{Bmatrix}, \tag{27}$$

where

$$\mathbf{M} = \begin{bmatrix}1 & 0 \\ 0 & 0\end{bmatrix}; \mathbf{C} = \begin{bmatrix}2\zeta\omega_n + (1-a)\omega_n^2 C_1 & 0 \\ C_3 & 1\end{bmatrix}; \mathbf{K} = \begin{bmatrix}a\omega_n^2 & (1-a)\omega_n^2 C_2 \\ 0 & C_4\end{bmatrix}. \tag{28}$$

Next, the response power spectrum matrix of the system of Eqs. (27) is expressed as

$$\mathbf{B}(\omega) = \begin{bmatrix}B_{xx}(\omega) & B_{xz}(\omega) \\ B_{zx}(\omega) & B_{zz}(\omega)\end{bmatrix} = \mathbf{H}(\omega)\begin{bmatrix}G(\omega) & 0 \\ 0 & 0\end{bmatrix}\mathbf{H}^*(\omega), \tag{29}$$

in which

$$\mathbf{H}(\omega) = \begin{bmatrix} H_{xx}(\omega) & H_{xz}(\omega) \\ H_{zx}(\omega) & H_{zz}(\omega) \end{bmatrix} = \left(-\omega^2 \mathbf{M} + i\omega \mathbf{C} + \mathbf{K} \right)^{-1}, \tag{30}$$

and the superscripts (*) and (-1) stand for complex matrix transposition and matrix inversion, respectively. Then, the required response variances are determined from the elements of the matrix **B** using the equations [35]

$$\sigma_{\dot{x}}^2 = \int_0^\infty \omega^2 B_{xx}(\omega)\, d\omega = \int_0^\infty \omega^2 \left| \frac{i\omega + C_4}{\sum_{j=0}^{3} (i\omega)^j A_j} \right|^2 G(\omega)\, d\omega \approx \Delta\omega \sum_{k=0}^{N} \omega_k^2 \left| \frac{i\omega_k + C_4}{\sum_{j=0}^{3} (i\omega_k)^j A_j} \right|^2 G[\omega_k], \tag{31}$$

and

$$\sigma_z^2 = \int_0^\infty B_{zz}(\omega)\, d\omega = \int_0^\infty \left| \frac{-i\omega C_3}{\sum_{j=0}^{3} (i\omega)^j A_j} \right|^2 G(\omega)\, d\omega \approx \Delta\omega \sum_{k=0}^{N} \left| \frac{-i\omega C_3}{\sum_{j=0}^{3} (i\omega_k)^j A_j} \right|^2 G[\omega_k], \tag{32}$$

in which $i = \sqrt{-1}$, and

$$A_0 = a\omega_n^2 C_4 ; \quad A_1 = a\omega_n^2 + \left(2\zeta\omega_n + (1-a)\omega_n^2 C_1 \right) C_4 - (1-a)\omega_n^2 C_2 C_3 ; \\ A_2 = C_4 + 2\zeta\omega_n + (1-a)\omega_n^2 C_1 ; \quad A_3 = 1 \tag{33}$$

Finally, the cross-variance term appearing in Eqs. (21) to (25) is determined by the equation

$$E\{\dot{x}z\} = -\frac{C_4}{C_3}\sigma_z^2 . \tag{34}$$

The latter equation is derived by multiplying Eq. (20) by $z(t)$, taking the mathematical expectation and noting that $E\{\dot{z}(t)z(t)\} = 0$, since $z(t)$ is a stationary process. Note that the integrals appearing in the calculation of the response variances in Eqs. (31) and (32) can be approximated by a finite summation. This can be done by using the frequency domain discretization scheme introduced in the numerical evaluation of the input spectrum $G(\omega)$ at a set of ω_k frequencies (Eq. (9)).The accuracy of this approximation depends on the

discretization step $\Delta\omega$ and can be readily improved, at will, by straightforward interpolation schemes.

To this end, Eqs. (21)~(24), (31), (32), and (34) form a system of seven non-linear equations with seven unknowns, namely, C_1~C_4, $\sigma_{\dot{x}}^2, \sigma_z^2$, and $E\{\dot{x}z\}$. This system can be readily written as a standard minimization problem and solved numerically by any appropriate optimization routine starting from a reasonable initial guess. In all of the ensuing numerical work a built-in optimization algorithm of MATLAB$^{®}$ using a trust region dog-leg search method is used to solve the aforementioned system of equations [36]. Furthermore, standard MATLAB$^{®}$ built-in routines are used for the numerical evaluation of the error and complementary error functions (Eq. (26)), and of the integral appearing in Eq. (22). Alternatively, the latter integral can be evaluated at each iteration required by the optimization algorithm using the series expansion reported in [14].

Upon determination of the C_1 to C_4 coefficients, an "equivalent" linear third-order system (ELS) involving the x, $\dot{x}$, and z states is established governed by the differential Eqs. (19) and (20). Note that it has been established in the literature [12,14-16], both theoretically and through numerical experimentation, that this ELS captures the response statistics of bilinear hysteretic systems exhibiting strong nonlinear behavior more accurately than a second-order ELS derived by the statistical linearization approach due to Caughey [12,13]. However, this third order ELS cannot be readily related to a response/design spectrum pertaining to the peak response of linear SDOF oscillators. To this end, in the next section a novel approach to reduce the system order is introduced by relying on a specific statistical criterion.

4.   Derivation of effective linear properties from the 3rd order equivalent linear system

Let y be the normalized by x_y deformation of an "auxiliary" linear SDOF oscillator of critical viscous damping ζ_{eff} and natural frequency ω_{eff} base excited by the acceleration process $g(t)$. The governing equation of motion of this auxiliary system reads as

$$\ddot{y}(t) + 2\zeta_{eff}\omega_{eff}\dot{y}(t) + \omega_{eff}^2 y(t) = -g(t)/x_y, \tag{35}$$

and zero initial conditions apply. For the purposes of this work, it is desired to relate the above second order linear system to the third order ELS of Eqs. (19) and (20). This can be accomplished by enforcing equality of the stationary variances of the processes $x(t)$ and $y(t)$. That is,

$$\sigma_x^2 = E\left\{x(t)^2\right\} = \int_0^\infty \frac{G(\omega)/x_y^2}{\left(\omega^2 - \omega_{eff}^2\right)^2 + \left(2\zeta_{eff}\omega_{eff}\omega\right)^2} d\omega = \lambda_{eff,0,G}/x_y^2; \tag{36}$$

and of the stationary variances of the processes $\dot{x}(t)$ and $\dot{y}(t)$, that is,

$$\sigma_{\dot{x}}^2 = \int_0^\infty \frac{\omega^2 G(\omega)/x_y^2}{\left(\omega^2 - \omega_{eff}^2\right)^2 + \left(2\zeta_{eff}\omega_{eff}\omega\right)^2} d\omega = \lambda_{eff,2,G}/x_y^2. \tag{37}$$

The variance appearing in the lhs of Eq. (36) can be calculated by the expression

$$\sigma_x^2 = \int_0^\infty \left|\frac{i\omega + C_4}{\sum_{j=0}^3 (i\omega)^j A_j}\right|^2 G(\omega)d\omega \approx \Delta\omega \sum_{k=0}^N \left|\frac{i\omega_k + C_4}{\sum_{j=0}^3 (i\omega_k)^j A_j}\right|^2 G[\omega_k]. \tag{38}$$

At this stage, the coefficients C_1 to C_4 are known from solving the nonlinear system of equations considered in the statistical linearization solution of the previous section. Thus, σ_x^2 is readily calculated numerically in the same manner as the variances in Eqs. (31) and (32). The variance appearing in the lhs of Eq. (37) is also a known quantity from the solution of the aforementioned system of equations. In this regard, Eqs. (36) and (37) define a system of two

nonlinear equations which can be solved for the two unknown effective linear properties ζ_{eff} and ω_{eff} corresponding to the considered auxiliary linear SDOF oscillator. To this aim, the same optimization algorithm used to obtain the statistical linearization solution can be employed. At each iteration of the optimization algorithm, the expressions included in the Appendix A are used to numerically evaluate the integrals in Eqs. (36) and (37) in a computationally efficient manner.

Note that in computing the response variances appearing in Eqs. (36)~(38) the fact that the duration T_s of the stationary process $g(t)$ is finite has not been explicitly taken into account. However, as already suggested in section 2, it is possible to consider a long enough duration T_s in deriving the response spectrum compatible power spectrum $G(\omega)$ so that the effective pair of properties $T_{eff} = 2\pi/\omega_{eff}$ and ζ_{eff} correspond to a point on the plots of Fig. 2 for which the corrective damping defined in Eq. (3) coincides with the value of ζ_{eff}. That is, exp(-2 ζ_{eff} ω_{eff} T_s)≈0. Under this condition, it can be argued that the transient nature of the input process $g(t)$ does not need to be taken into account and one can treat the response statistics of the linear systems defined by Eqs. (19) and (20), and by Eq. (35) as being stationary. Additional comments on this issue are provided in a following section in light of numerical data corresponding to a large range of bilinear hysteretic systems.

5.   Peak nonlinear response estimation using the effective linear properties

The preceding three sections provided the theoretical background to derive effective linear properties (ELPs) (ζ_{eff} and ω_{eff}) for viscously damped bilinear hysteretic systems exposed to a given code-prescribed elastic response pseudo-acceleration spectrum $S_\alpha(T,\zeta)$ following the proposed approach outlined in Fig. 1. The salient advantage of this approach is that these ELPs depend not only on the properties of the nonlinear systems considered, namely, damping ζ, pre-yield natural frequency ω_n, yielding displacement x_y, and rigidity

ratio α, but also to the specified response spectrum $S_a(T,\zeta)$ [10,11]. In this regard, it can be argued that a reasonable estimate of the peak deformation of bilinear hysteretic oscillators can be determined by the expression

$$\max_t \left\{ |x(t)| \right\} \approx \frac{S_a\left(T_{eff}, \zeta_{eff}\right)}{\omega_{eff}^2} = B\left(T_{eff}, \zeta_{eff}\right) \frac{S_a\left(T_{eff}, \zeta = 5\%\right)}{\omega_{eff}^2} . \tag{39}$$

That is, by using a family of response spectra corresponding to various damping ratios. Such response spectra are commonly defined in most of the earthquake resistant design applications by means of multiplying a "reference" design spectrum corresponding to $\zeta = 5\%$ by a reduction factor B. In general, it is known that this factor depends on the damping ratio and on the natural period of oscillation, and, thus, on the ELPs as suggested in the last equation (see e.g. [9,37]). In this manner, the need for numerically integrating the non-linear Eqs. (15) and (16) of motion for an ensemble of seismic accelerograms compatible with the considered response/design spectrum is by-passed.

Obviously, the reliability of the estimated peak value will depend on the severity of the nonlinear response induced by the seismic action. Further, it will reflect the well-quantified approximations associated with the statistical linearization method [12,15]. Also, it will depend on the effectiveness of the adopted B factor to predict the peak response of linear SDOF oscillators for different ratios of critical damping which remains an issue of open research [9,37]. To this end, it is noted that in case dependable response spectra are not available for damping ratios other than ζ, an estimate of the peak non-linear response can be achieved by the equation

$$\max_t \left\{ |x(t)| \right\} \approx \eta_{eff} \sigma_x , \tag{40}$$

which relies on the concept of the peak factor and the fact that the variance of $x(t)$ has been set equal to the variance of $y(t)$ in Eq. (36). In the last equation, η_{eff} can be calculated from

Eqs. (1)~(8) by setting $p=0.5$, $\zeta=\zeta_{eff}$, and $\omega_j=\omega_{eff}$ and by considering the power spectrum $G(\omega)$ and the duration T_s used to obtain the ζ_{eff} and ω_{eff} pair of ELPs.

6. Numerical application to the EC8 design spectrum

6.1 EC8 compatible effective linear properties of bilinear hysteretic systems

The elastic response (uniform hazard) spectrum of the current aseismic code provisions effective in Europe (EC8) [2] is considered herein as a paradigm of assessing the usefulness and applicability of the proposed approach. Specifically, the EC8 (target) pseudo-acceleration response spectrum for peak ground acceleration 0.36g (g= 981cm/sec^2), ground type "B" and damping ratio ζ= 5% (gray thick line in Fig. 4(a)), is considered to represent the induced seismic action. The broken line of Fig. 4(b) corresponds to a discrete power spectrum compatible with the considered EC8 target spectrum computed by means of Eq. (9) assuming T_s= 20s, $\Delta\omega$= 0.1rad/s, and using Eqs. (11) and (12) to estimate the peak factors η_k. Further, this initial power spectrum is modified by performing four iterations using Eq. (14). The obtained modified spectrum is also shown in Fig. 4(b). The pseudo-acceleration response spectra associated with the two power spectra of Fig. 4(b) are plotted in Fig. 4(a) and compared with the target spectrum. These response spectra have been calculated analytically using Eqs. (1)~(8). It can be seen that the response spectrum corresponding to the initial power spectrum cannot trace closely the target spectrum near the "corner period" of 0.5s which signifies the end of the flat segment of constant spectral ordinates. However, the iteratively matched power spectrum characterized by a quite prominent spike at a frequency of $2\pi/0.5$= 12.6 rad/s yields a significantly better matching with the target spectrum along the whole axis of natural periods. This is further confirmed by considering the median spectral ordinates of an ensemble of 2000 20s long stationary signals compatible with the iteratively modified spectrum (plotted as dots in Fig. 4(a)). These signals have been generated using a

random field simulation technique based on an auto-regressive-moving-average filter [38]. The latter Monte Carlo-based simulation analysis ensures numerically that the criterion prescribed by Eq. (4) for $p=0.5$ is satisfied by the iteratively modified spectrum considered.
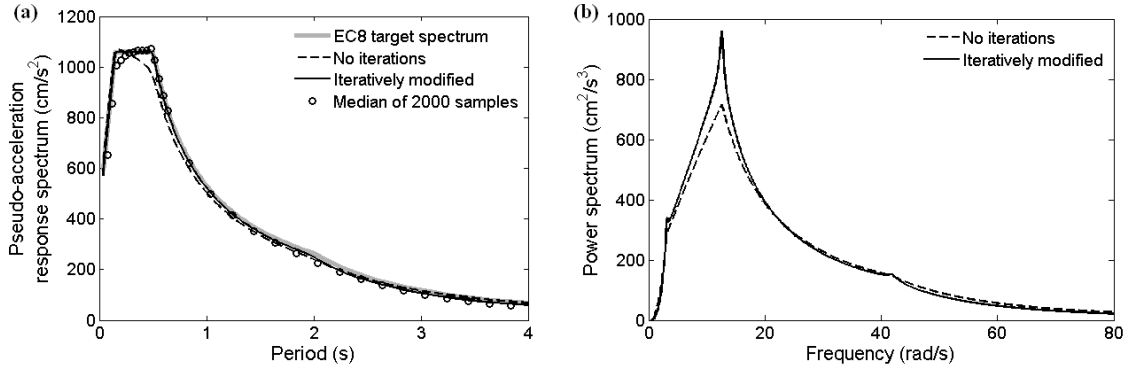
Fig. 4 (a) Target EC8 spectrum, response spectra corresponding to the power spectra shown in panel (b) and median response spectrum from 2000 simulated signals. (b) Power spectra compatible with the EC8 spectrum of panel (a).

Next, the iteratively modified power spectrum of Fig. 4(b) is used to obtain effective linear properties (ELPs) $T_{eff}= 2\pi/\omega_{eff}$ and ζ_{eff} via the statistical linearization-based method detailed in sections 3 and 4 for various bilinear hysteretic oscillators. In particular, the seven-by-seven system of nonlinear Eqs. (21)~(24), (31), (32), and (34) is solved in series with the two-by-two system of nonlinear Eqs. (36) and (37) for viscously damped bilinear oscillators with $\zeta=5\%$, pre-yield natural period $T_n=0.5s$, 1.0s, 1.5s, and 2s ($T_n= 2\pi/\omega_n$), rigidity ratios α ranging from 0.5 to 0.05 and for several values of yielding deformation x_y. The latter is treated as the "free" parameter to represent different levels of nonlinear behavior. The thus obtained ELPs are plotted in Fig. 5 against the "ductility" $\max|y|$ defined in Eq. (35) which quantifies the severity of the nonlinear response. These data serve to provide numerical evidence that the herein proposed approach yields results that are in reasonable agreement with engineering intuition.

In general, the departure from the linear response quantified by larger values of max|y|

yields "softer" effective linear systems characterized by longer natural periods. It is noted,

however, that the ratio of T_{eff}/T_n is not quite sensitive to changes in the pre-yield stiffness for

a fixed rigidity α and ductility level (panels (a) and (c) in Fig. 5). This ratio appears to be

more influenced by the rigidity α and increases at a significantly higher rate, as max|y|

increases for bilinear systems closer to the ideal elasto-plastic one, that is, as $\alpha \rightarrow 0$ (panels (e)

and (g) in Fig. 5). Accordingly, the effective damping ratio increases with max|y| to account

for the increased energy dissipation through more severe plastic/ hysteretic behavior of the

corresponding nonlinear systems. Similar trends for ELPs of bilinear hysteretic oscillators

subject to white noise excitation have been reported in the literature [e.g. 13, 39].

Notably, it is observed that for all bilinear systems considered herein, reflecting a large

range of systems pertinent to earthquake engineering applications, ζ_{eff} increases quite rapidly

with ductility and at a much higher rate than T_{eff}. Consequently, in all cases plotted in Fig. 5

the product $\omega_{eff}\zeta_{eff}$ tend to increase as stronger nonlinear behaviour is exhibited. It turns out

that the quantity $\exp(-2\zeta_{eff}\,\omega_{eff}\,T_s)$ for T_s=20s negligible in all cases considered in Fig. 5.

Thus, by referring to Fig. 2, it is suggested that for bilinear systems with ζ=5% viscous

damping and $T_n \leq 2$s choosing a duration of at least T_s=20s in deriving the response spectrum

compatible power spectrum $G(\omega)$ circumvents the need to consider the transient nature of the

response moments appearing in Eqs. (36)~(38). In this regard, the underlying process $g(t)$ can

be treated as stationary in the context of the proposed approach of Fig. 1. Clearly, if bilinear

systems with smaller than 5% ratio of viscous damping are considered, a longer duration may

be required to be adopted in treating $g(t)$ as stationary. If for any practical reason this is not

possible, then the transient nature of the response moments in Eqs. (36)~(38) can be

accounted for by similar steps as those delineated in section 2. That is, by considering an

increased fictitious damping ratio dependent on the duration and the natural frequency of the considered linear systems [19,22,23].

Note that in obtaining the plots in Fig. 1, the ductility $\max|y|$ has been estimated for each pair of effective linear properties by using the considered EC8 elastic spectrum without performing any numerical integration as detailed in the next sub-section.
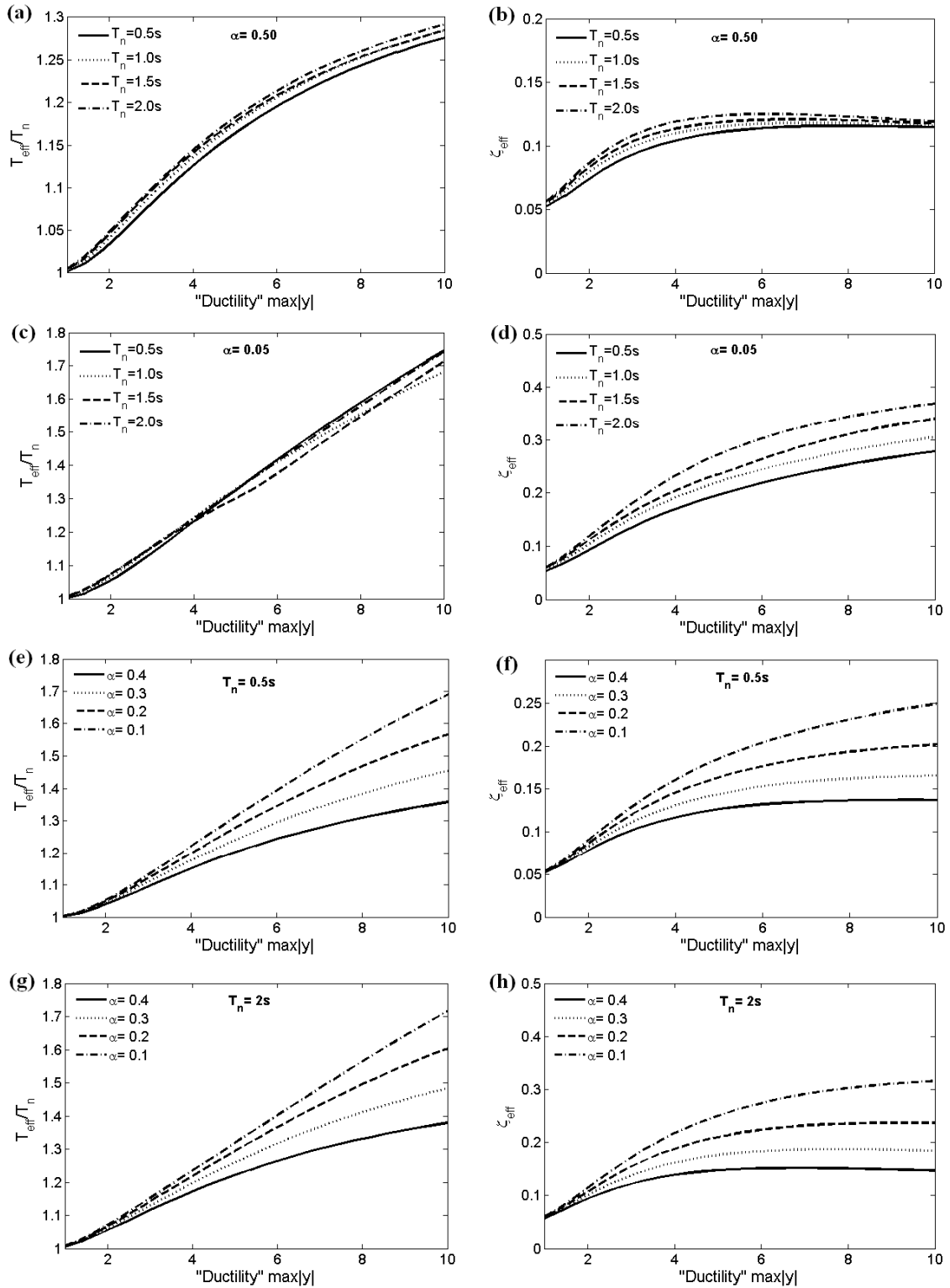
Fig. 5 Effective linear properties for various bilinear hysteretic systems.

6.2 Estimation of peak nonlinear response using the effective linear properties

In the preceding sub-section ELPs (ζ_{eff} and ω_{eff}) have been derived for several viscously damped bilinear hysteretic systems exposed to the EC8 response spectrum of Fig. 4(a) following the proposed approach outlined in Fig. 1. From the discussion included in section 5 it is clear that these ELPs can be used in conjunction with the EC8 spectrum to estimate the peak nonlinear response of the considered systems. This is done by substituting in Eq. (39) the B factor for $T=T_{eff}$ and $\zeta=\zeta_{eff}$ prescribed by EC8 which for ground type "B" reads as [2]

$$
B_{EC8}(T,\zeta) = \begin{cases} \dfrac{1+\dfrac{T}{0.15}\left(2.5\sqrt{\dfrac{10}{5+\zeta}}-1\right)}{1+10T} \; ; 0 \leq T \leq 0.15 \\ \sqrt{\dfrac{10}{5+\zeta}} \; ; 0.15 \leq T \leq 4 \end{cases}, \tag{41}
$$

where ζ needs to be expressed as a percentage (i.e. $\zeta \to 5$ for $\zeta = 5\%$). The aforementioned nonlinear peak response estimation step can perhaps be better understood graphically as shown in Fig. 6 in terms of deformations (panels (b) and (d)) and in terms of psedo-acceleration (panels (a) and (c)) for various bilinear hysteretic systems. In particular, consider a specific viscously damped bilinear hysteretic oscillator with damping ratio $\zeta = 5\%$ and pre-yield natural period T_n exposed to the EC8 elastic response spectrum (vertical broken lines). One can move, following the horizontal arrows, to a vertical solid line corresponding to an effective linear system characterized by T_{eff} and ζ_{eff} obtained by the statistical linearization based methodology herein adopted and "read" the related spectral ordinate. In this manner, an estimate of the peak response of the considered structural system is achieved without the need to have available suites of spectrum compatible accelerograms and to numerically integrate the governing nonlinear equation of motion.
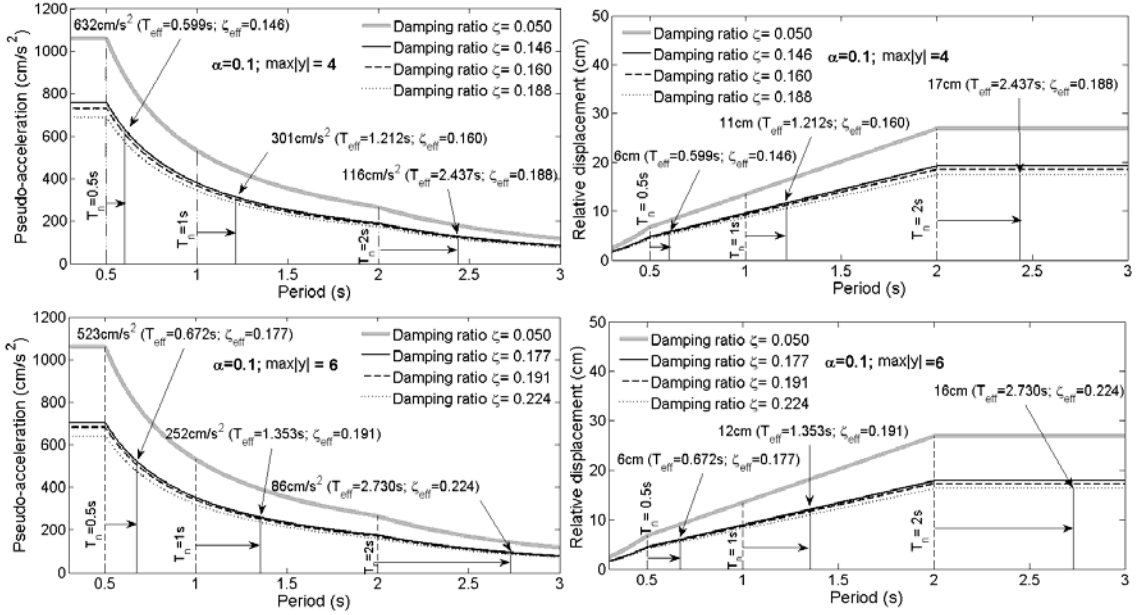
Fig. 6 Peak response estimation using the effective linear properties in conjunction with the EC8 elastic spectrum for various values of damping.

As a final note, it is pointed out that the "ductility" in the plots of Fig. 5 and Fig. 6 has been computed by

$$\max\left\{\left|y\left(t\right)\right|\right\} = B_{EC8}\left(T_{eff}, \zeta_{eff}\right) \frac{S_a\left(T_{eff}, \zeta = 5\%\right)}{x_y \omega_{eff}^2}.$$ (42)

6.3 Assessment of peak nonlinear response predictions via Monte Carlo simulation

In this section the potential of the EC8 compatible ELPs plotted in Fig. 5 to provide reasonable estimates of the peak response of the corresponding bilinear hysteretic systems is assessed in a Monte Carlo simulation context. To this aim, an ensemble of 250 artificial non-stationary accelerograms compatible with the EC8 spectrum of Fig. 4(a) are considered. These signals have been generated by a wavelet-based stochastic approach recently proposed by Giaralis and Spanos [40]. The time-history of an arbitrarily chosen accelerogram is plotted in Fig. 7 along with its velocity and displacement trace. Furthermore, pertinent statistics of the spectral ordinates of the considered accelerograms in terms of displacement and pseudo-

acceleration are included on the same figure and compared with the target EC8 spectrum. In particular, the average response spectrum of the 250 considered accelerograms practically coincides with the EC8 spectrum. Thus, these signals are consistent with the compatibility criterion utilized in deriving the input power spectrum $G(\omega)$ (see also Fig. 4) considered in obtaining the ELPs of Fig. 5.
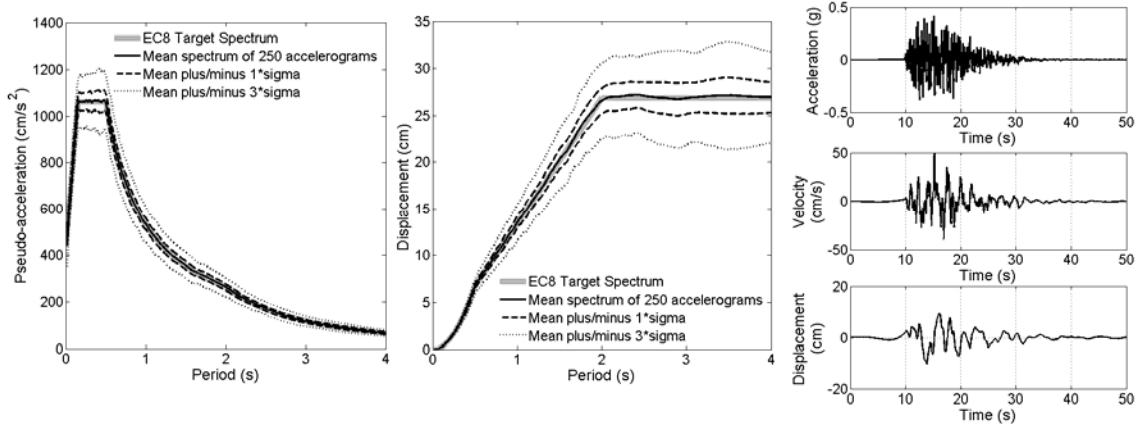
Fig. 7 Response spectra statistics and time-history traces of a sample of 250 non-stationary artificial accelerograms compatible with the EC8 spectrum of Fig. 4(a).

Next, the aforementioned accelerograms are used to excite various bilinear hysteretic systems. The nonlinear response is obtained by numerical integration of the nonlinear Eqs. (15) and (16). The standard constant acceleration Newmark's scheme, incorporating an iterative Newton-Raphson algorithm to treat locally the discontinuities of the piecewise linear force-deformation law, is used for the task [3]. In Fig. 8 the ductility of certain bilinear systems (dots of various shapes) computed from ensemble averaging of the systems' nonlinear responses is plotted versus the strength reduction factor R (R-μ-T_n relationships); R is defined in Fig. 3(b) as the ratio of the peak demand in terms of elastic restoring force f_{el} for a particular excitation over the yielding strength f_y of the bilinear oscillator. In the same figure the, thus, obtained R-μ-T_n relationships are examined vis-à-vis the peak response normalized by the yielding deformation x_y (max|y|) of effective linear oscillators (curves of various kinds)

whose properties (ELPs) have been derived as detailed in the previous sub-section from the considered nonlinear systems.

In general, the quality of the achieved approximation of the peak nonlinear responses by the peak responses of the corresponding heavily damped linear oscillators deteriorates as the level of nonlinear behavior increases. That is, for smaller rigidity ratios α and for larger strength reduction factors R. This is expected and reflects the approximations involved in the statistical linearization step discussed in section 3 (see also [12,13]).

Overall, satisfactory matching of the average peak values for the considered ensemble of accelerograms is achieved for bilinear hysteretic systems of rigidity ratios as small as α=0.1~0.2 and for a wide range of strength reduction factors (Fig. 8 (a) and (b)). Further, Fig. 8(c) provides a comparison of the accuracy achieved between the herein proposed approach and the earlier one of Giaralis and Spanos [11] which utilizes a second-order statistical linearization scheme based on the work of Caughey [13]. The latter is computationally less involved, requiring the solution of only one three-by-three system of nonlinear equations. However, the herein proposed approach yields significantly better results for bilinear systems with relatively small rigidity ratios and thus stronger nonlinear response.
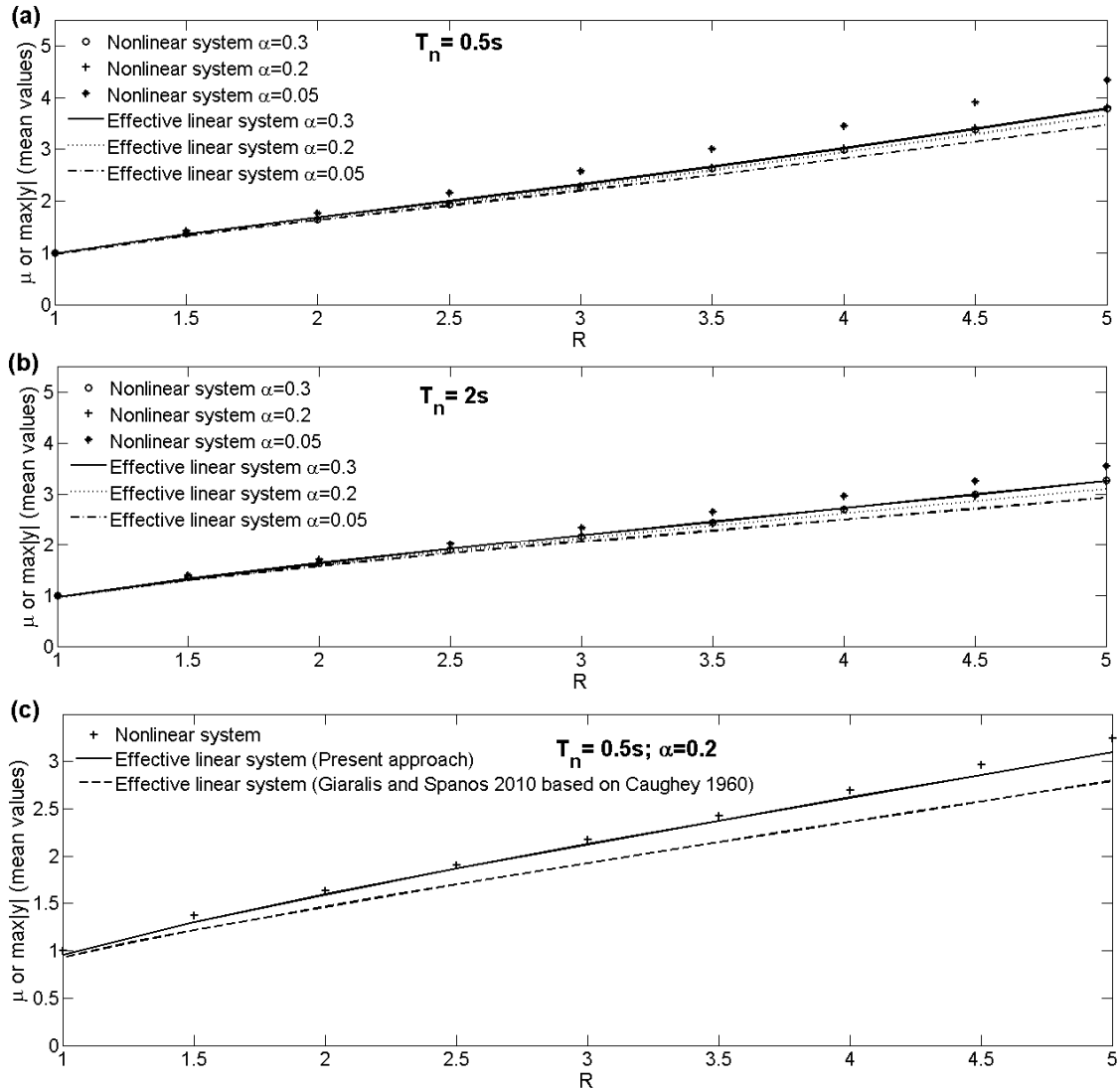
Fig. 8 Mean peak responses of various bilinear hysteretic and of their corresponding effective linear systems subject to the 250 EC8 compatible accelerograms considered in Fig. 7.

7. Concluding Remarks

A novel statistical linearization based approach has been proposed for deriving effective linear properties (damping ratio and natural frequency) (ELPs) corresponding to linear SDOF oscillators for viscously damped bilinear SDOF hysteretic systems subject to seismic excitation defined by a response/design spectrum. These ELPs are determined by solving one seven-by-seven system and one two-by-two system of non-linear equations. The first system of equations provides a frequency domain statistical linearization solution which

replaces the bilinear system by a third order linear system. The second system of equations is associated with a system reduction step to capture certain of the response statistics of the third order linear system by a second order SDOF oscillator response statistics. Both solutions involve the employment of a numerically derived power spectrum representing in the frequency domain a "quasi-stationary" process of finite duration satisfying a certain probabilistic compatibility criterion with the given response spectrum. This criterion conforms with common aseismic code provisions for acceleration time-histories. That is, the average response spectrum of samples belonging to the considered process is close to the given response (uniform hazard) spectrum. An efficient recursive formula has been used to determine the required power spectrum satisfying the aforementioned compatibility criterion. A salient feature of the thus obtained ELPs is that they are explicitly associated with both the pre-specified response spectrum and the considered bilinear system. In this respect, it is possible to obtain reliable estimates of the peak nonlinear response by utilizing the ELPs in conjunction with the given elastic response spectrum modified appropriately to account for different values of damping ratio. In this manner, the peak nonlinear response is obtained from heavily damped elastic response spectra without integrating the nonlinear equations of motion. This is done without considering ensembles of response spectrum compatible scaled/modified field recorded and/or artificially generated accelerograms. The potential of the ELPs to serve this purpose has been ascertained by pertinent numerical results associated with the elastic response uniform hazard spectrum prescribed by the aseismic code regulations effective in Europe (EC8). Specifically, EC8 compatible ELPs corresponding to various bilinear systems of different rigidity ratios, pre-yield stiffness, and yielding deformations have been obtained. Further, strength reduction-ductility-natural period (R-μ-T-$_n$) relationships have been derived for the considered hysteretic systems and for the associated effective linear ones within a Monte Carlo based analyses pertaining to an ensemble of 250

EC8 compatible non-stationary time-histories obtained via a wavelet-based stochastic approach. For these time-histories reliable estimates of the nonlinear average peak response have been obtained for rigidity ratios of the order of 10~20% and for strength reduction factors of the order of 5. In this regard, it has been demonstrated that the proposed approach which employs a high-order (third-order) statistical linearization technique and a novel order reduction step provides significantly better compared to the earlier work of the authors in [11] estimates of the peak inelastic response of bilinear inelastic/hysteretic oscillators exhibiting strong nonlinear behavior. Further, the developed approach can potentially be modified to accommodate versatile smooth nonlinear systems whose hysteretic component can be represented by means of an additional differential equation, such as the Bouc-Wen model [41].

Appendix A.

Consider a power spectrum G corresponding to a quasi-stationary stochastic process known at a set of discrete equally spaced frequencies ω_q, that is $G[\omega_q] = G_q$, where $\omega_q = \omega_0 + (q-0.5)\Delta\omega$, with $q = 1,2,\ldots,M$ and ω_0 is given by Eq (10). Using the "grid" $\omega_p = \omega_0 + (p-1)\Delta\omega$; $p = 1,2,\ldots,M+1$, to discretize the frequency axis, the first three response spectral moments of Eqs. (1)~(3) can be numerically evaluated using the formula [30]

$$\lambda_{n,m,G} = \sum_{p=1}^{M} J_{n,m,p} G_p, \qquad (A)$$

in which

$$
\begin{aligned}
J_{n,m,p} = &\frac{x_1}{2}\ln\frac{\left(\omega_{p+1}-\omega_D\right)^2+c^2}{\left(\omega_p-\omega_D\right)^2+c^2} + \\
&\frac{x_2+\omega_D x_1}{c}\left\{\frac{\pi}{2}\left[1-\mathrm{sgn}\left(\frac{c\left(\omega_{p+1}-\omega_p\right)}{\left(\omega_{p+1}-\omega_D\right)\left(\omega_p-\omega_D\right)+c^2}\right)\right]+\tan^{-1}\frac{c\left(\omega_{p+1}-\omega_p\right)}{\left(\omega_{p+1}-\omega_D\right)\left(\omega_p-\omega_D\right)+c^2}\right\} + \\
&\frac{x_3}{2}\ln\frac{\left(\omega_{p+1}-\omega_D\right)^2+c^2}{\left(\omega_p-\omega_D\right)^2+c^2}+\frac{x_4-\omega_D x_3}{c}\tan^{-1}\frac{c\left(\omega_{p+1}-\omega_p\right)}{\left(\omega_{p+1}+\omega_D\right)\left(\omega_p+\omega_D\right)+c^2}
\end{aligned} \qquad (B)
$$

where $\omega_D = \omega_n \sqrt{1 - \zeta_n^2}$, $c = \omega_n \zeta_n$, and

$$\begin{Bmatrix} x_1 \\ x_2 \\ x_3 \\ x_4 \end{Bmatrix} = \begin{bmatrix} -\dfrac{1}{4\omega_n^2 \omega_D} & 0 & \dfrac{1}{4\omega_D} \\[2ex] \dfrac{1}{2\omega_n^2} & \dfrac{1}{4\omega_D} & 0 \\[2ex] \dfrac{1}{4\omega_n^2 \omega_D} & 0 & -\dfrac{1}{4\omega_D} \\[2ex] \dfrac{1}{2\omega_n^2} & -\dfrac{1}{4\omega_D} & 0 \end{bmatrix} \begin{Bmatrix} r_0 \\ r_1 \\ r_2 \end{Bmatrix} \quad ; \quad r_i = \begin{cases} 1, i = m \\ 0, i \neq m \end{cases}. \qquad (C)$$

References

[1] McGuire RK. Seismic Hazard and Risk Analysis. Monograph MNO-10. Oakland: Earthquake Engineering Research Institute; 1995.

[2] CEN. Eurocode 8: Design of Structures for Earthquake Resistance - Part 1: General Rules, Seismic Actions and Rules for Buildings. EN 1998-1: 2004. Brussels: Comité Européen de Normalisation; 2004.

[3] Chopra AK. Dynamics of Structures. Theory and Applications to Earthquake Engineering. 2nd ed. Englewood Cliffs: Prectice-Hall; 2001.

[4] Veletsos AS, Newmark NM. Response spectra for single-degree-of-freedom elastic and inelastic systems. Rep. No.RTD-TDR-63-3096. Vol. III. Albuquerque: Air Force Weapons Laboratory; 1964.

[5] Chopra AK, Chintanapakdee C. Inelastic deformation ratios for design and evaluation of structures: Single-degree-of-freedom bilinear systems. J Struct Eng ASCE 2004;130: 1309-19.

[6] Miranda E, Ruiz-García J. Evaluation of approximate methods to estimate maximum inelastic displacement demands. Earthquake Eng Struct Dyn 2002;31:539-60.

[7] Levy R, Rutenberg A, Qadi Kh. Equivalent linearization applied to earthquake excitations and the R-μ-T_o relationships. Eng. Struct 2006;28:216-28.

[8] Kwan WP, Billington SL. Influence of hysteretic behavior on equivalent period and damping of structural systems. J Struct Eng ASCE 2003;129:576-85.

[9] Lin YY, Miranda E. Evaluation of equivalent linear methods for estimating target displacements of existing structures. Eng Struct 2009;31:3080-89.

[10] Spanos PD, Giaralis A. Statistical linearization based analysis of the peak response of inelastic systems subject to the EC8 design spectrum. In: Santini A, Moraci N, editors. Proceedings of the 2008 Seismic Engineering International Conference commemorating the 1908 Messina and Reggio Calabria Earthquake, New York: American Institute of Physics; 2008, Vol 2, p. 1236-44.

[11] Giaralis A, Spanos PD. Effective linear damping and stiffness coefficients of nonlinear systems for design spectrum based analysis. Soil Dyn Earthquake Eng 2010;30:798-810.

[12] Roberts JB, Spanos PD. Random Vibration and Statistical Linearization. New York: Dover Publications; 2003.

[13] Caughey TK. Random excitation of a system with bilinear hysteresis. J Appl Mech ASME 1960;27:649-52.

[14] Asano K, Iwan WD. An alternative approach to the random response of bilinear hysteretic systems. Earthquake Eng Struct Dyn 1984;12:229-36.

[15] Spanos PD, Kougioumtzoglou IA. Harmonic wavelets based statistical linearization for response evolutionary power spectrum determination. Probab Eng Mech 2012;27:57-68.

[16] Lutes LD, Sarkani S. Random Vibrations: Analysis of Structural and Mechanical Systems. Oxford: Butterworth-Heinemann; 2004.

[17] Naess A. Prediction of extreme response of nonlinear structures by extended stochastic linearization. Probab Eng Mech 1995;10:153-160.

[18] Fujimura K, Der Kiureghian A. Tail-equivalent linearization method for nonlinear random vibration. Probab Eng Mech 2007;22:63-76.

[19] Vanmarcke EH. Structural Response to Earthquakes. In: Lomnitz C, Rosenblueth E, editors. Seismic Risk and Engineering Decisions, Amsterdam: Elsevier; 1976.

[20] Cacciola P, Colajanni P, Muscolino G. Combination of modal responses consistent with seismic input representation. J Struct Eng ASCE 2004;130:47-55.

[21] Park YJ. New conversion method from response spectrum to PSD functions. J Eng Mech ASCE 1995;121:1391–2.

[22] Gupta ID, Trifunac MD. Defining equivalent stationary PSDF to account for nonstationarity of earthquake ground motion. Soil Dyn Earthquake Eng 1998;17:89-99.

[23] Kaul MK. Stochastic characterization of earthquakes through their response spectrum. Earthquake Eng Struct Dyn 1978;6:497-509.

[24] Der Kiureghian A. Structural response to stationary excitation. J Eng Mech Div ASCE 1980;106:1195-1213.

[25] Corotis RB, Vanmarcke EH, Cornell CA. First passage of nonstationary random processes. J Eng Mech Div ASCE 1972;98:401-14.

[26] Spanos PD. Non-stationary random vibration of a linear structure. Int J Solids Struct 1978;14:861-867.

[27] Spanos PD, Lutes LD. Probability of response to evolutionary process. J Eng Mech Div ASCE 1980;106:213-224.

[28] Michaelov G, Lutes LD, Sarkani S. Extreme value of response to nonstationary excitation. J Eng Mech ASCE 2001;127:352-63.

[29] Giaralis A, Spanos PD. Derivation of response spectrum compatible non-stationary stochastic processes relying on Monte Carlo-based peak factor estimation. Earthquakes Struct 2012;3:581-609.

[30] Di Paola M, La Mendola L. Dynamics of structures under seismic input motion (Eurocode 8). Eur. Earthquake Eng 1992;6(II):36-44.

[31] Priestley MJN, Calvi GM, Kowalsky MJ. Displacement-Based Seismic Design of Structures. Pavia: IUSS Press; 2007.

[32] Suzuki Y, Minai R. Application of stochastic differential equations to seismic reliability analysis of hysteretic structures. Probab Eng Mech 1998;3:43-52.

[33] Atalik TS, Utku S. Stochastic linearization of multi-degree-of-freedom non-linear systems. Earthquake Eng. Struct. Dyn., 19764, 411-20.

[34] Kazakov IE. Generalization of the method of statistical linearization to multidimensional systems. Automat Rem Cont,1965 26, 458-64.

[35] Giaralis A. Wavelet based response spectrum compatible synthesis of accelerograms and statistical linearization based analysis of the peak response of inelastic systems. Houston: Ph.D. Thesis, Department of Civil and Environmental Engineering, Rice University; 2008.

[36] Nocedal J, Wright SJ. Numerical Optimization. New York: Springer-Verlag; 1999.

[37] Hubbard DT, Mavroeidis GP. Damping coefficients for near-fault ground motion response spectra. Soil Dyn Earthquake Eng 2011;31:401-17.

[38] Spanos PD, Zeldin BA. Monte Carlo treatment of random fields: A broad perspective. Appl Mech Rev 1998;51:219-37.

[39] Lutes LD. Equivalent linearization for random vibration. J Eng Mech Div ASCE 1970;96:227-242.

[40] Giaralis A, Spanos PD. Wavelets based response spectrum compatible synthesis of accelerograms- Eurocode application (EC8). Soil Dyn Earthquake Eng 2009;29:219-35.

[41] Wen YK. Equivalent linearization for hysteretic systems under random excitation. J Appl Mech ASME 1980;47:150-4.